

Numerical study on the importance of radiative heat transfer in building energy simulation

W. C. Tam^a, W. W. Yuen^b and W. K. Chow^a

^aDepartment of Building Services Engineering, The Hong Kong Polytechnic University, Hung Hom, Kowloon, Hong Kong, China; ^bDepartment of Mechanical Engineering, University of California at Santa Barbara, Santa Barbara, CA, USA

ABSTRACT

A neural network-based model for interior longwave radiative heat transfer has been developed and implemented into a new computer code, BERHT (Building Energy with Radiative Heat Transfer). The model accounts for the non-gray effect of absorbing species in a building environment and the geometric effect of a three-dimensional building structure. Numerical studies have been carried out on a rectangular single-story building. For nominal concentration of CO₂, H₂O, and small particulates, results show that the effect of radiative heat transfer is important. The surface emissivity of enclosure walls and optical properties of the absorbing/emitting medium are demonstrated to have significant effects on the distribution of heat transfer between convection and radiation, as well as the transient behavior of the indoor air temperature. Supplemental studies provide an insight that the one-zone, well-mixed model used in building energy simulation generates a "fictitious" non-local heat transfer behavior, leading to uncertainties in the understanding of the radiative heat transfer effect.


ARTICLE HISTORY

Received 10 May 2015
Accepted 18 July 2015

Introduction

Improving energy efficiency in buildings has been identified as a key step by many nations, including the U.S. and China, in achieving the goal of energy efficiency and the reduction of greenhouse gas (CO₂, CH₄, NO₂, etc.) emissions. In the U.S., the building sector accounts for 40% of the total energy consumption [1]. In China, this figure is about 23% and the number is observed to be increasing in recent years [2]. These statistics indicate a vital need to improve building energy performance. A great deal of effort has thus been reported in developing computational tools for effective simulation of building energy transport [3, 4].

While many building energy simulation programs have been developed over the past decades (BLAST, DeST, DOE-2, ECOTECH, IES <VE>, EnergyPlus, TAS, and TRNSYS) and many of them have implemented highly sophisticated models for conductive and convective heat transfer [5, 6], the modeling of radiative heat transfer has largely been treated in a highly simplified and ad hoc level with uncertain accuracy. For example, in DeST [7], DOE-2.2 [8], ECOTECH [9], and TRNSYS 17 [10], radiative heat flux is represented by a linearized effective heat transfer coefficient and the view factor is evaluated approximately by an area ratio. In TAS [11] and IES <VE> [12], radiative heat transfer is modeled by a mean radiant temperature model with a coupling coefficient. The exact view factor is used while the effect of gray surfaces is accounted for by the Oppenheim surface resistance concept [13]. In

CONTACT W. C. Tam  andy.tam@connect.polyu.hk  Department of Building Services Engineering, The Hong Kong Polytechnic University, Hung Hom, Kowloon, Hong Kong, China.

Color versions of one or more of the figures in the article can be found online at www.tandfonline.com/unht.

This work was partly presented at the 11th AIAA/ASME Joint Thermophysics and Heat Transfer Conference, AIAA Aviation, Atlanta, GA, June 2014.

© 2016 Taylor & Francis

Nomenclature

| | | | |
|----------------------|---|---------------------|--|
| Symbols | | Q_g | = total radiative heat transfer to medium due to both surface and mixture emission |
| A_i ($i = 1, 6$) | = bounding areas of building structure | $Q_{w, i}$ | = radiative heat transfer on surface A_i due to surface emission only |
| c_p | = specific heat of air or air mixture | Q_{sys} | = HVAC system output |
| h_{conv} | = convective heat transfer coefficient | Q_{load} | = sum of internal convective loads |
| \dot{m}_{inf} | = mass flow rate due to infiltration of outside air | $S_i S_j$ | = exchange factors |
| N_{load} | = total number of internal convective loads | T_g | = temperature of medium |
| N_{surf} | = total number of interior surfaces | T_w | = temperature of interior surface |
| q''_{cond} | = conduction heat flux | T_z | = temperature of zone air |
| q''_{conv} | = convective flux exchange | σ | = Stefan-Boltzmann constant |
| q''_{rad} | = longwave radiative flux exchange | ε_i | = emissivity of surface A_i |
| q''_{sol} | = absorbed direct and diffuse solar radiation heat flux (shortwave) | ρ_{air} | = density of air |
| q''_{source} | = sum of heat gains from lights, people, and equipment | V_z | = volume of zone air in the building structure |
| $q_{o,i}$ | = radiosity from surface A_i | Subscripts | |
| $q_{og,i}$ | = radiosity from surface A_i due to mixture emission only | ext | = exterior surfaces of the building structure |
| Q_i | = total radiative heat transfer on surface A_i due to both surface and mixture emission | int | = interior surfaces of the building structure |
| | | Superscripts | |
| | | wall | = emission due to surface only |
| | | gas | = emission due to mixture only |

EnergyPlus v.8 [14], a net radiation method is implemented to account for the effect of diffuse gray surfaces. However, in all of these existing models, except for IES <VE> in which the emissivity of the medium is simulated by an empirical correlation [12], the effect of the participating (absorbing and/or emitting) medium is completely neglected due to mathematical complexity in modeling the non-gray effect in a three-dimensional building structure [15–18] and assumption of low concentration in participating components (CO_2 , H_2O , and small particulates) and their short mean path-lengths [14, 19].

The lack of motivation in developing a more realistic radiative transfer model in building energy simulation programs is driven by the general expectation that at low temperatures, the effect of radiation is not significant compared with convection in a building structure [20]. However, there has been no rigorous verification of this expectation, particularly in view of the uncertain accuracy of the radiation model in the existing building energy simulation programs.

In a recent work [21], a computationally efficient approach is developed for the evaluation of the total absorptivity of a one-dimensional slab of combustion mixture (CO_2 , H_2O , and small particulates in which the size of particles satisfies the Rayleigh small-particle absorption limit) using narrow-band absorption data [22]. Specifically, numerical data for the total absorptivity, generated by a direct integration of the spectral data, are correlated by a neural network, RAD-NETT, as a function of the relevant physical parameters such as source temperature, absorption gas temperature, partial pressures, and particulate volume fraction. Based on RAD-NETT, the analysis of radiative heat transfer in a three-dimensional geometry using the realistic spectral data is now possible. The relevant surface–surface and surface–volume exchange factors for a specific geometry, generated by direct numerical integration, are further correlated by additional neural networks [23, 24]. In the present work, based on zonal analysis, the neural network based radiation model is developed and implemented into a newly developed computer code, BERHT (Building Energy with Radiative Heat Transfer). Numerical results are generated and the effect of interior longwave radiative heat transfer is assessed for a considered geometry in a building environment in developing computational tools for effective simulation of building energy transport [3, 4].

Development of BERHT

BERHT is a thermal building simulation program and it is developed based on the existing whole-building energy simulation software, EnergyPlus. BERHT and EnergyPlus use the same heat transfer models and calculation algorithms, and the core of the simulation modeling is primarily based on the

principle of heat balance. With the implementation of the neural network-based radiation model, BERHT is capable of performing energy simulation in the presence of an absorbing/emitting non-gray medium. Therefore, it can be used to study the effect of thermal processes, to simulate energy flows, and to evaluate the heating and cooling energy consumption for a one-zone building structure with the effect of participating media.

Mathematical formulation

Energy balance

To formulate the heat balance equations, a building structure is considered as an enclosure bounded by a number of discrete surfaces, such as walls, floors, ceilings, and windows. Based on the one-zone approximation described in reference [14], the indoor air is assumed to be well mixed. The thermal properties and temperature of the indoor air and the surrounding surfaces are considered to be uniform. At each boundary, heat flux entering the boundary must equal the heat flux leaving the boundary. Thus, on any interior surfaces of an enclosure, heat flow into the surfaces due to conductive heat flux is balanced by convection from the indoor air, net radiative flux exchange between the air and the interior surfaces, and heat gain from transmitted solar radiation and other internal sources such as lights, equipment, and occupants. Similarly, for exterior surfaces, absorbed solar radiation, net longwave radiation flux from the surroundings, and convective flux from the outdoor air are balanced by conductive flux entering the surface. In addition, a heat balance of the indoor air is required to describe the energy imbalance due to heat added from convective flux exchange from the interior surfaces, longwave radiation flux exchange from the interior surfaces and the indoor air, infiltration, and interior heat sources.

For exterior surfaces in a zone, the heat balance equation is written as:

$$q''_{\text{ext,sol}} + q''_{\text{ext,conv}} + q''_{\text{ext,rad}} - q''_{\text{ext,cond}} = 0 \quad (1)$$

and for interior surfaces:

$$q''_{\text{int,cond}} + q''_{\text{int,conv}} + q''_{\text{int,rad}} + q''_{\text{int,sol}} + q''_{\text{source}} = 0 \quad (2)$$

where q''_{source} is the sum of the heat gains from lights, equipment, and people. The heat transfer models used to evaluate the terms in Eqs. (1) and (2) are identical to the EnergyPlus except that a new model is developed for the evaluation of radiation exchange in the interior. The radiation model algorithm for the new radiation model will be described in the next subsection and the detailed explanation for the other heat transfer models can be found in reference [14].

The heat balance for the indoor air/zone air can be written as the change in energy stored in indoor air equal to the sum of internal schedule convective loads, convection to interior surfaces, infiltration, system output, and radiation to interior surfaces:

$$\rho_{\text{air}} c_p V_z \frac{dT_z}{dt} = \sum_{i=1}^{N_{\text{load}}} Q_{\text{load},i} + \sum_{i=1}^{N_{\text{surf}}} h_{\text{conv},i} A_i (T_{w,i} - T_z) + \dot{m}_{\text{inf}} c_p (T_{\text{air}} - T_z) + Q_{\text{sys}} + Q_{\text{g}} \quad (3)$$

where N_{load} is the total number of internal convective loads, N_{surf} is the total number of interior surfaces, and Q_{rad} is the new radiation term. Note that the modeling algorithms for the calculation of the internal convective loads, convective heat transfer coefficient, mass flow rate of air due to infiltration, and HVAC system output are explained in detail in the EnergyPlus engineering document [14].

Radiation model algorithm

In a one-zone model, even the temperature and radiative properties are assumed to be uniform in the enclosure interior, and radiative heat transfer is three-dimensional. To incorporate the geometry effect, various exchange factors must be evaluated for the considered enclosure. Specifically, the

exchange factor between two surfaces is given by:

$$S_i S_j = \int_{A_i} \int_{A_j} \frac{[1 - \alpha(T_w, T_g, P_g L, F_{CO_2}, f_v L)] \cos \theta_i \cos \theta_j}{\pi L^2} dA_i dA_j \quad (4)$$

where L is the line-of-sight distance between the two integration area elements dA_i and dA_j ; θ_i and θ_j are the angles between the line-of-sight and the unit normal vector of the two differential area elements; T_w is the temperature of the emitting wall, and A_i and T_g the temperature of the absorbing gas; f_v is the particle volume fraction and P_g is the total partial pressure of the absorbing gas. The evaluation of the total absorptivity, α , using the neural network RAD-NETT and the formulation of the exchange factors, $S_i S_j$, are presented in references [21] and [23, 24], respectively.

With the tabulated exchange factors, radiative heat exchange in the enclosure interior can be determined. Since the exchange factors depend on both wall temperature (T_w) and medium/gas mixture temperature (T_g), separate analyses are needed to determine the incident heat flux due to the emission from the different surfaces and that due to the gas mixture (indoor air), which are emitting at different temperatures. A superposition procedure is therefore needed to simulate the radiative heat transfer. Specifically, a zonal analysis is carried out for one hot (emitting) surface (A_i), with emissivity ε_i , maintained at temperature $T_{w,i}$ while the remaining surfaces are assumed to be non-emitting but reflecting ($T_{w,j} = 0, j \neq i$), with an emissivity of ε_j . The medium is assumed to be absorbing and non-emitting maintained at temperature T_g . Assuming that all surfaces are diffuse, the relevant equations generated from the zonal analysis [25] are:

$$\frac{(\sigma T_{w,i}^4 - q_{o,i}) A_i \varepsilon_i}{(1 - \varepsilon_i)} = A_i q_{o,i} - \sum_{k \neq i} S_i S_k (T_{w,i}, T_g) q_{o,k} \quad (5)$$

$$\frac{(-q_{o,j}) A_j \varepsilon_j}{(1 - \varepsilon_j)} = A_j q_{o,j} - \sum_{k \neq j} S_j S_k (T_{w,i}, T_g) q_{o,k} \quad (6)$$

Note that in Eqs. (4) and (5), all the exchange factors are evaluated at a wall temperature of $T_{w,i}$ and a medium (indoor air) temperature of T_g . Thus, the heat transfer on different surfaces, A_j , due to emission from a hot surface, A_i , is given by:

$$Q_{w,j,i}^{\text{wall}}(T_{w,i}, T_g) = \sum_{k \neq j} S_j S_k (T_{w,i}, T_g) q_{o,k} - A_j q_{o,j}, j = 1, 6 \quad (7)$$

and the heat transfer to the absorbing and non-emitting medium due to emission from the hot surface, A_i , is:

$$Q_{g,i}^{\text{wall}}(T_{w,i}, T_g) = \sum_{i=1}^6 \left[A_i - \sum_{j \neq i} S_i S_j (T_{w,i}, T_g) \right] q_{o,i} \quad (8)$$

where $S_i S_j$ is the exchange factor between two surfaces. Repeating the application of Eqs. (6) and (7), the heat transfer on different surfaces due to emission from all hot surfaces is:

$$Q_{w,i}^{\text{wall}} = \sum_{j=1}^6 Q_{w,i,j}^{\text{wall}}(T_{w,j}, T_g) \quad (9)$$

and the heat transfer to the absorbing and non-emitting medium is:

$$Q_g^{\text{wall}} = \sum_{k=1}^6 Q_{g,k}^{\text{wall}}(T_{w,k}, T_g) \quad (10)$$

To account for the mixture emission, a further analysis is carried out for an absorbing and emitting medium with reflecting but non-emitting surfaces. The relevant equation is:

$$\frac{(-q_{og,i})A_i\varepsilon_i}{(1-\varepsilon_i)} = A_iq_{og,i} - \sum_{j \neq i} S_i S_j(T_g, T_g)q_{og,j} - \sum_{j \neq i} [A_i F_{ij} - S_i S_j(T_g, T_g)] \sigma T_g^4 \quad (11)$$

for all absorbing, non-emitting surfaces ($i = 1, 6$). The heat transfer to the surface is now given by:

$$Q_{w,i}^{\text{gas}} = \sum_{k \neq i} S_i S_k(T_g, T_g)q_{og,k} - A_i q_{og,i} + \left[A_i - \sum_{j \neq i} S_i S_j(T_g, T_g) \right] \sigma T_g^4 \quad (12)$$

and the heat transfer to the medium is:

$$Q_g^{\text{gas}} = \sum_{i=1}^6 \left[A_i - \sum_{j \neq i} S_i S_j(T_g, T_g) \right] [q_{og,i} - \sigma T_g^4] \quad (13)$$

By superposition, the total heat transfer on each surface due to both surface and gas mixture emission is:

$$Q_i = Q_{w,i}^{\text{wall}} + Q_{w,i}^{\text{gas}} = q''_{\text{int,rad},i} A_i \quad (14)$$

and the total heat transfer to the medium is:

$$Q_g = Q_g^{\text{wall}} + Q_g^{\text{gas}} \quad (15)$$

where $q''_{\text{int,rad},i}$ is the interior longwave radiative flux exchange on surface A_i .

It should be noted that the zonal analysis using the concept of radiosity for gray surfaces is an approximation (since the radiosity is generally non-uniform across the surface) for a gray medium and finite surfaces. For a non-gray medium, the current zonal analysis introduces another layer of approximation since the reflection from a surface does not have the same spectral dependence of the original blackbody source at temperature T_w . For engineering applications such as the current one-zone approximation, this approach is expected to be sufficiently accurate to demonstrate the parametric behavior of the various enclosure parameters. Direct assessment of the accuracy of the method (by taking smaller discrete areas and breaking up the wavelength spectrum into multiple bands with constant absorption coefficient) is current under consideration and will be presented in future applications.

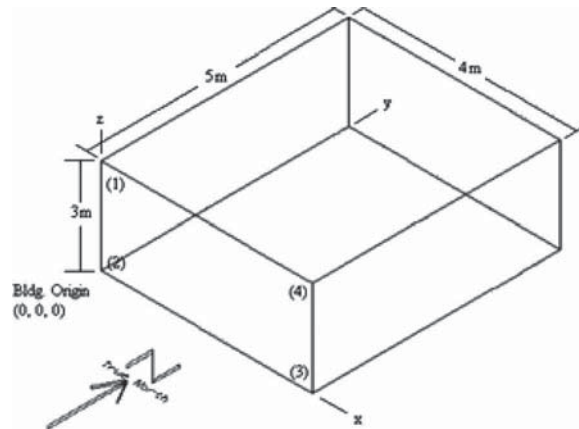


Figure 1. Geometry of building enclosure.

Table 1. Construction of building envelopes.

| Name | North surface | East surface | South surface | West surface | Floor surface | Roof surface |
|---------|---------------|--------------|---------------|--------------|---------------|--------------|
| Layer 1 | WS – 1 | WS – 1 | WS – 1 | WS – 1 | HF – C5 | Roof deck |
| Layer 2 | FQ – 1 | FQ – 1 | FQ – 1 | FQ – 1 | na | FQ – 2 |
| Layer 3 | PB – 1 | PB – 1 | PB – 1 | PB – 1 | na | PB – 2 |

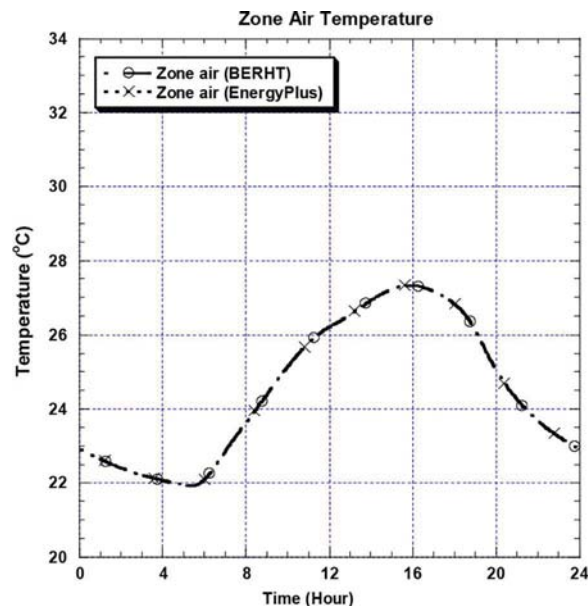
Note that WS, FQ, and PB denote wood sliding, fiberglass quilt, and plasterboard, respectively.

Table 2. Material properties.

| | Units | Object 1 | Object 2 | Object 3 | Object 4 | Object 5 | Object 6 | Object 7 |
|---------------------|-------------------|---------------|----------|----------|----------|----------|-----------|--------------|
| Name | | PB – 1 | FQ – 1 | WS – 1 | PB – 2 | FQ – 2 | Roof deck | HF – C5 |
| Roughness | – | Medium Smooth | Rough | Rough | Rough | Rough | Rough | Medium rough |
| Thickness | m | 0.012 | 0.066 | 0.009 | 0.01 | 0.1119 | 0.019 | 0.1015 |
| Conductivity | W/m-K | 0.16 | 0.04 | 0.14 | 0.16 | 0.04 | 0.14 | 1.7296 |
| Density | kg/m ³ | 950 | 840 | 530 | 950 | 12 | 530 | 2,243 |
| Specific heat | J/kg-K | 840 | 840 | 900 | 840 | 840 | 900 | 837 |
| Thermal absorptance | – | 0.9 | 0.9 | 0.9 | 0.9 | 0.9 | 0.9 | 0.9 |
| Solar absorptance | – | 0.6 | 0.6 | 0.6 | 0.6 | 0.6 | 0.6 | 0.65 |

Numerical study

Numerical studies are conducted on a test building, as shown in Figure 1, which is a rectangular single-zone building with dimensions of 4 m × 5 m × 3 m. The building is constructed with six surfaces and is simulated as located in Chicago, IL on a typical summer day (July 21). All exterior surfaces, except the floor surface, are exposed to varying temperature from outdoor air, solar radiation from the sun, forced convection due to wind, and thermal radiation exchange with the surroundings. These outdoor conditions are obtained analytically using the algorithms described in reference [14] with the weather profile. The floor surface is maintained at a constant temperature of 22.3°C. For interior surfaces, each surface is exposed to natural convective heat exchange with the zone (indoor) air and longwave radiative heat exchange between the other interior surfaces

**Figure 2.** Comparison of zone air temperature for a case without a participating medium (BERHT and EnergyPlus).

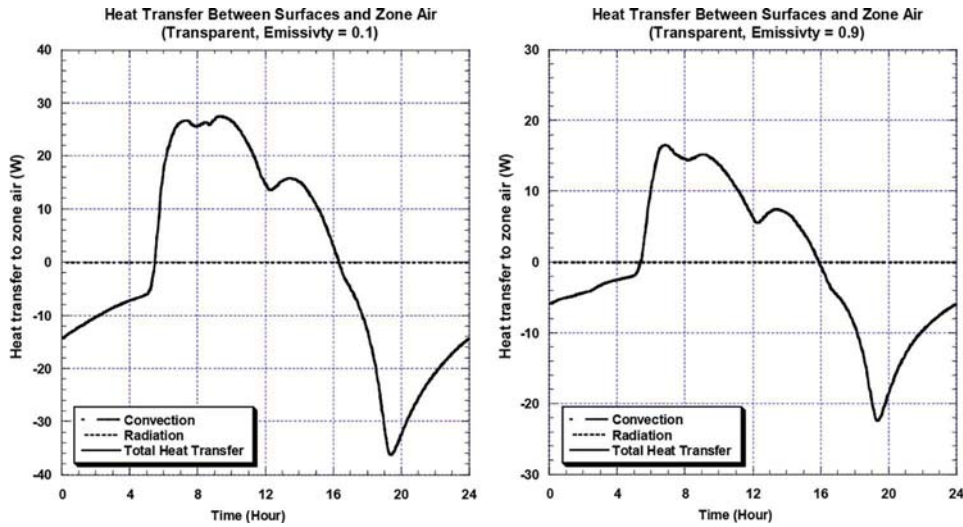


Figure 3. Heat transfer (radiation, convection, and total) between surfaces and room air with a transparent medium for 2 different emissivity cases.

and the zone air. In this numerical study, the zone air is considered to be an absorbing/emitting medium consisted of up to three species (H_2O , CO_2 , and small particulates).

Since our goal is to investigate the potential maximum radiative heat transfer effect in the participating medium, the studies are conducted with a fixed partial pressure of 5 kPa for both H_2O and CO_2 and a fixed volume fraction (0 or 10^{-6}) for the small particulates. For simplicity, the effects of infiltration, ventilation, and HVAC systems are not included in the current simulation. These simulation conditions are identical to a case study by EnergyPlus, for which the details of the location and the weather at the site can be found in [14]. BERHT can thus be benchmarked against EnergyPlus by running this case without the presence of participating medium. Note that the gas mixture partial pressures and the particulate volume fraction are higher than the typically expected values in an indoor environment.

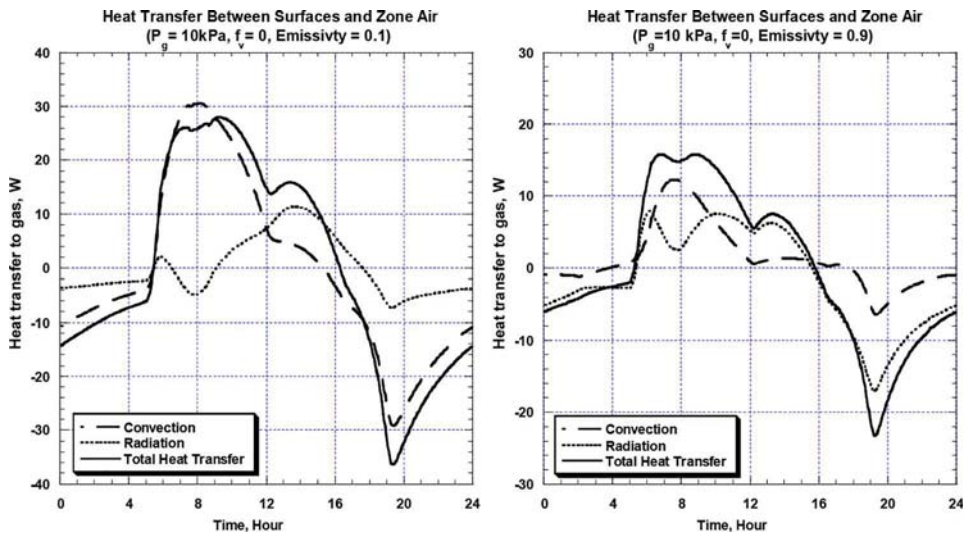


Figure 4. Heat transfer (radiation, convection, and total) between surfaces and room air with an absorbing/emitting gas-only mixture for two different emissivity cases.

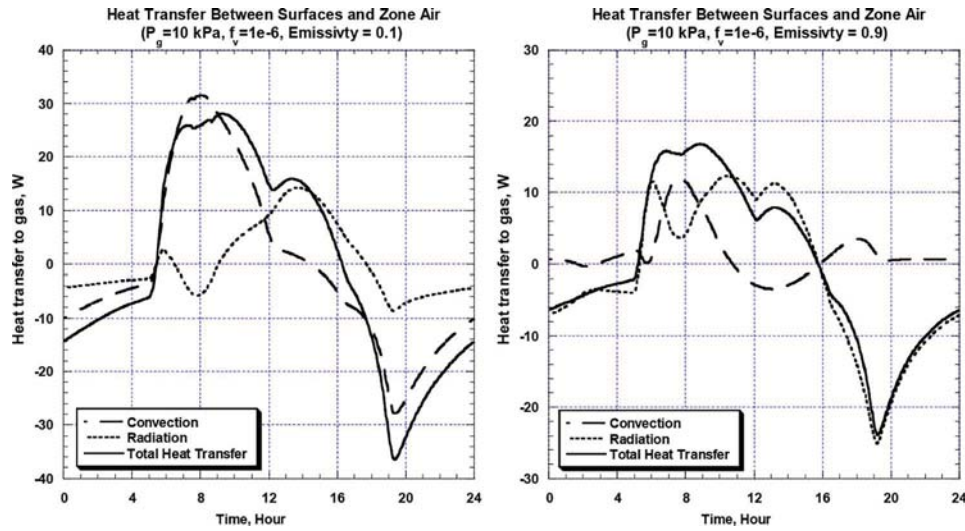


Figure 5. Heat transfer (radiation, convection, and total) between surfaces and interior air with an absorbing/emitting gas/particulates mixture for two different emissivity cases.

Construction of each surface and the thermal properties of material associated to each construction component are shown in Tables 1 and 2, respectively. For benchmarking purposes, Figure 2 shows the zone air temperature profile for the case with no participating medium. And as seen, excellent agreement is achieved between the EnergyPlus and BERHT.

Results and discussion

A series of numerical experiments were conducted to examine the importance of interior longwave radiative heat transfer and its effect on the overall heat transfer to zone air. Numerical data for the heat transfer to the medium in three cases (transparent, absorbing/emitting gas-only mixture, and absorbing/emitting gas/particulate mixture) are presented in Figures 3–5, respectively. The total convective heat transfer, total radiative heat transfer, and the overall heat transfer (the total convective

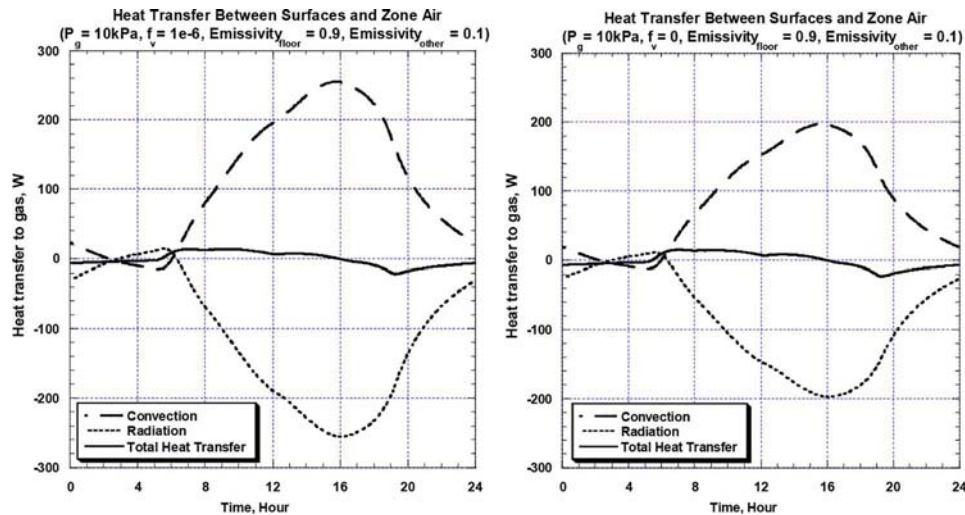


Figure 6. Heat transfer (radiation, convection, and total) between surfaces and room air in a mixed emissivity case ($\epsilon_{\text{floor}} = 0.9$ and $\epsilon_{\text{other}} = 0.1$) with two different absorbing/emitting mixture medium.

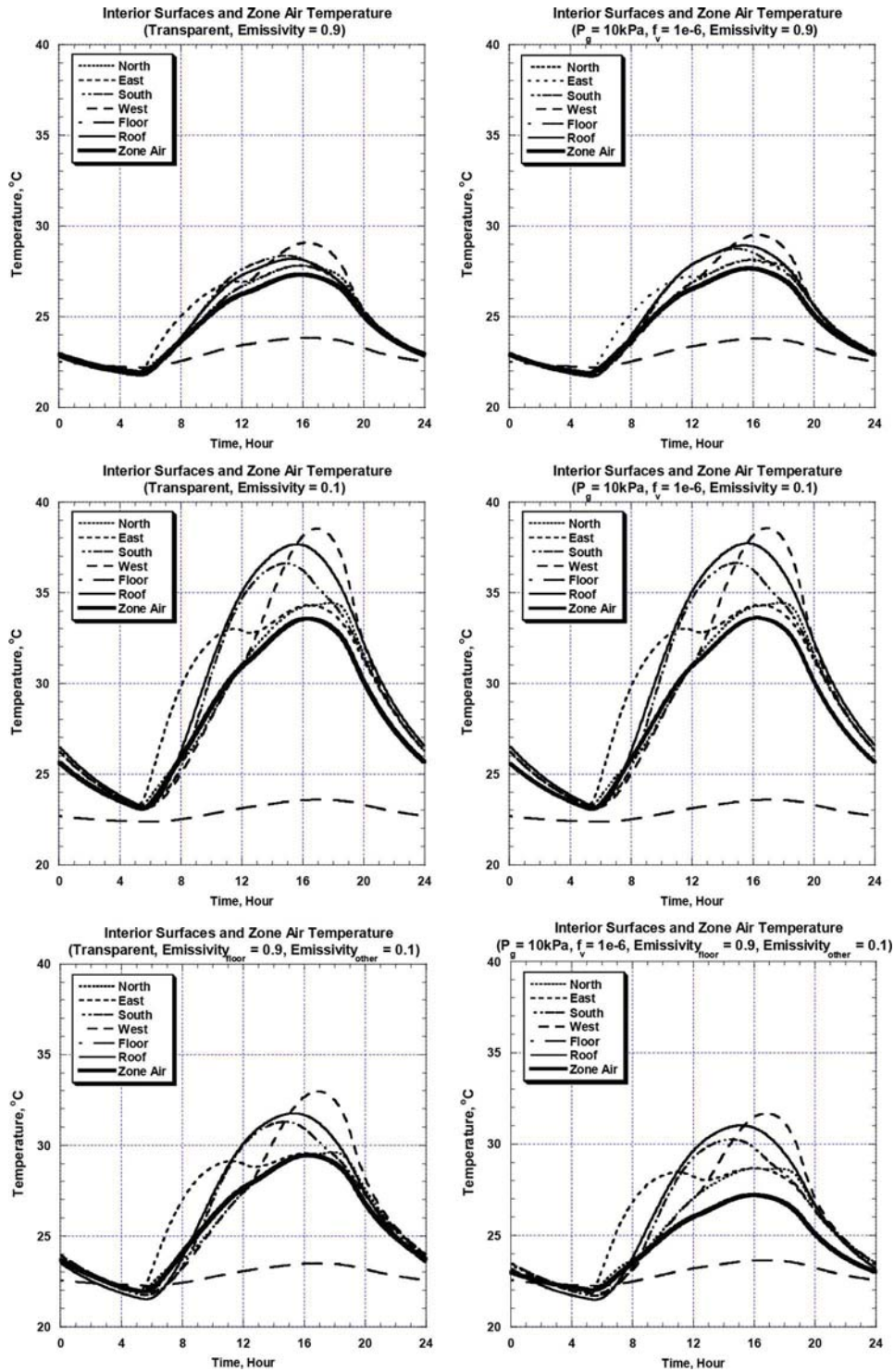


Figure 7. Comparison of the temperature at the different surfaces and the zone air temperature for cases with different emissivity (transparent versus absorbing/emitting gas/particulates mixture medium).

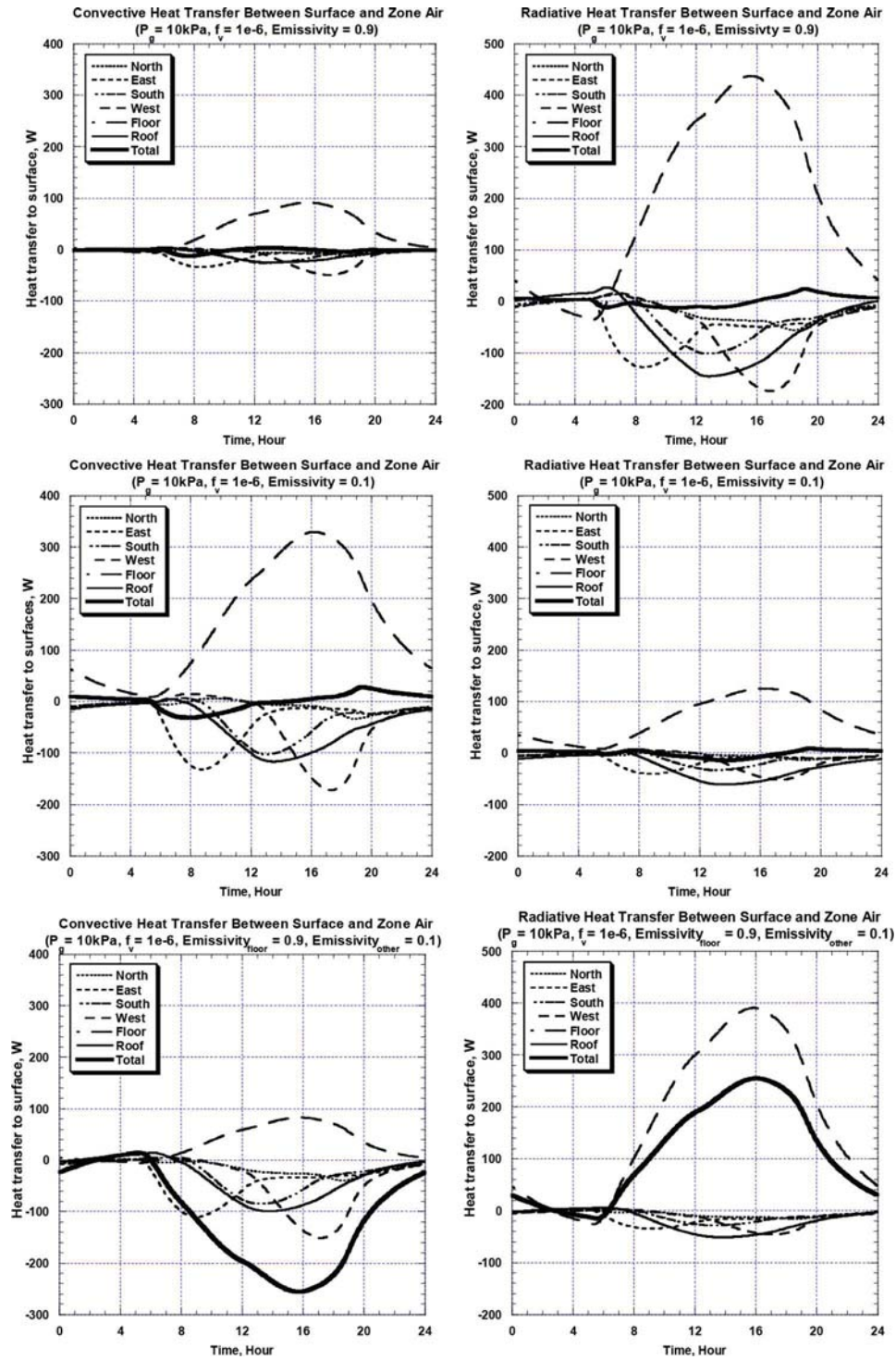


Figure 8. Comparison of the convective and radiative heat transfer from the different surfaces to the zone air for cases with different emissivity with an absorbing/emitting gas/particulates mixture.

heat transfer together with the total radiative heat transfer) between the surfaces and the zone air are shown to illustrate the effect of radiative heat transfer. Numerical data are also generated separately for two different interior surface configurations (emissivity = 0.9 and = 0.1, which are assumed to be identical for all interior surfaces). It is interesting to note that the presence of a participating medium (Figures 4 and 5) has no significant impact on the overall heat transfer to the zone air. Both with and without particulates, the increase in radiative heat transfer appears to be compensated by a reduction in convective heat transfer, while maintaining the same magnitude of the overall heat transfer.

To further investigate the effect of surface emissivity on the influence of the effect of radiative heat transfer and to illustrate how radiation heat transfer will impact the individual distribution between radiative and convective heat transfer, simulations were conducted with the floor surface emissivity parameterized to 0.9 and the emissivity of remaining surfaces maintained at 0.1 (mixed emissivity case). This case is selected to maximize the radiative heat loss from the medium and the floor (with the high absorptivity of the floor) and the heat absorption by the medium from the hot wall (with the high reflectivity from the wall). As expected, in terms of the individual convective and radiative heat transfer, significant differences are found in Figure 6. The high absorptivity of the floor results in a large heat radiative heat loss to the lower wall. The reduced zone air temperature, on the other hand, results in a large convective heat transfer from the surrounding hot walls.

The overall heat transfer between the surfaces and the zone air and the temperature profile for three different media are shown in Figure 7. The added effect of radiative heat transfer appears to have impact on the overall heat transfer and the zone air temperature distribution. Comparing the case with a transparent medium to that of a sooty gas/mixture medium, a maximum difference of 30% in overall heat transfer is observed and this results in a corresponding 2.5°C difference in temperature distribution. The transient temperature and corresponding heat transfer along the six walls for the two cases shown in Figures 3–6 are presented in Figures 8 and 9. In Figure 8, it is apparent that the surface emissivity has a strong effect on the temperature distribution of the different walls. Except for the floor which is an effective heat sink, lower emissivity leads to a higher wall temperature. The reduction in emissivity leads to a reduction in radiative heat flux as shown in Figure 9, but the increased wall temperature leads to a corresponding increase in the convective heat flux. Radiative heat transfer appears to be dominated by the surface-to-surface exchange and the effect of the participating medium is relatively small.

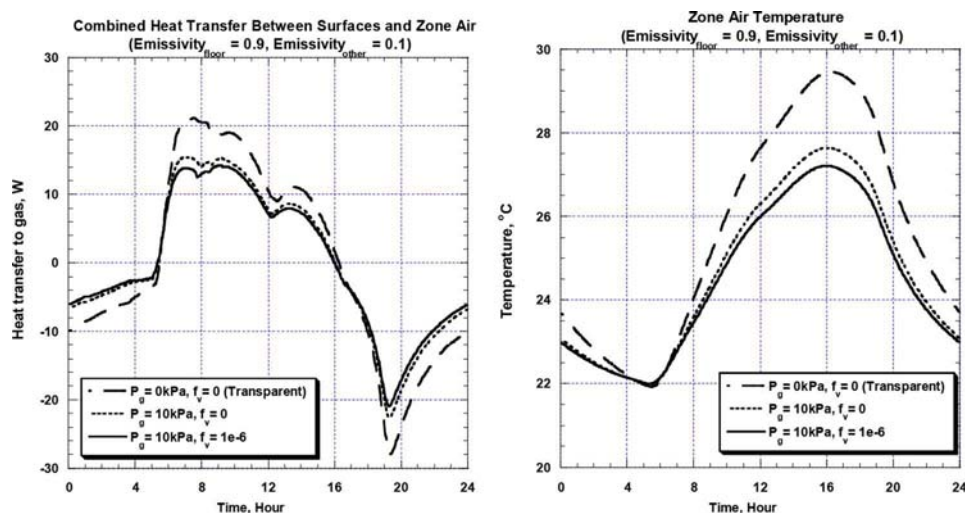


Figure 9. Heat transfer to the zone air (left) and zone air temperature (right) with 3 different medium for the mixed emissivity case ($\epsilon_{\text{floor}} = 0.9$ and $\epsilon_{\text{other}} = 0.1$).

The apparent lack of impact of radiative heat transfer on the overall heat transfer profile and the zone air temperature distribution can be attributed to two fundamental factors:

1. The well-mixed approximation of the one-zone model overpredicts the effect of convective heat transfer during the transient. The effect of radiation is thus erroneously included in codes such as EnergyPlus and BERHT, even in the transparent case. This phenomenon is demonstrated in Appendix A, in which the results generated by BERHT are compared to those generated without the well-mixed approximation obtained from Fluent.
2. In a one-zone model, the zone temperature represents the energy content of the zone air, which is controlled largely by external heat transfer and boundary conditions such as solar radiation, wind speed, and outside temperature. The specification of the exact heat transfer mechanism for convective and radiative heat transfer will only affect the distribution of heat transfer between the two mechanisms and the transient behavior. This effect is demonstrated in Appendix B.

In summary, radiative heat transfer effect is important even in a low-temperature environment typically encountered in building energy analysis. The surface emissivity of the enclosure walls and the optical properties of the absorbing/emitting medium have important effects on the distribution of heat transfer between convection and radiation, as well as the transient behavior of the temperature.

Conclusion

This study demonstrates the use of a neural network for the evaluation of thermal radiative heat transfer in a rectangular-shaped building structure in the presence of an isotropic homogenous absorbing/emitting medium. The neural network is shown to be an efficient tool to facilitate the realistic absorption/emission effect of a medium incorporated accurately and efficiently in heat transfer calculation for a three-dimensional building structure. With the implementation of the neural network exchange factors, a neural network-based one-zone net radiative exchange model is developed. Together with the new radiation model, a computer code BERHT is developed to simulate and understand the thermal radiative heat transfer effect in a low-temperature building structure environment.

Studies have been carried out for two different interior emissivity surfaces. Results show that the presence of participating medium has a significant effect on the distribution of total heat transfer between convection and radiation. The effect of radiation is important and is of the same order of magnitude as convection. However, the overall energy balance is influenced strongly by external conditions such as surrounding temperatures, exterior convective heat transfer, and shortwave and longwave radiation. Supplemental studies provide an insight that the convection models used in a building energy simulation program with the one-zone approximation overpredict the effect of convective heat transfer.

References

- [1] L. Pérez-Lombard, J. Ortiz, and C. Pout, A Review on Buildings Energy Consumption Information, *Energy Build.*, vol. 40, no. 3, pp. 394–398, 2008.
- [2] J. Liang, B. Li, W. Yong, and R. Yao, An Investigation of the Existing Situation and Trends in Building Energy Efficiency Management in China, *Energy Build.*, vol. 39, no. 10, pp. 1098–1106, 2007.
- [3] S. Pless, M. Deru, B. Griffith, N. Long, and R. Judkoff, Lessons Learned from Case Studies of Six High-Performance Buildings, National Renewable Energy Laboratory, Golden, CO, 2006.
- [4] D. B. Crawley, J. W. Hand, M. Kummert, and B. T. Griffith, Contrasting the Capabilities of Building Energy Performance Simulation Programs, *Build. Environ.*, vol. 43, no. 4, pp. 661–673, 2008.
- [5] WUFI, Version 2.2 Simultaneous Heat and Moisture Transport in Building Components, Fraunhofer IBP, Holzkirchen, Germany, 1999.
- [6] L. Peeters, I. Beausoleil-Morrison, and A. Novoselac, Internal Convective Heat Transfer Modeling: Critical Review and Discussion of Experimentally Derived Correlations, *Energy Build.*, vol. 43, no. 9, pp. 2227–2239, 2011.
- [7] DeST-h Technology Documents, Chap. 3, Tsinghua University, Beijing, China, 2004.

- [8] D. A. York and C. C. Cappiello, DOE-2 Engineers Manual Version 2.1A, Chap. 2, Lawrence Berkeley National Laboratory's Simulation Research 290 Group, University of California, Berkeley, CA, 1982.
- [9] N. Taylor, Energy Efficiency for Everyone: Analysis and Development of an Energy Efficient Project Home, B.S. thesis, Department of Environmental Engineering, The University of Western Australia, Australia, 2002.
- [10] TRNSYS 17 Documentation, Vol. 5, Chap. 5, University of Wisconsin-Madison, WI, 2013.
- [11] Thermal Analysis Software Theory Manual, Chap. 7, Environmental Design Solutions Limited, Milton Keynes, UK, 2010.
- [12] ApacheSim Calculation Methods <Virtual Environment> 6.3, Chap. 6, Integrated Environmental Solutions Limited, Glasgow, UK, 2010.
- [13] A. K. Oppenheim, Radiation Analysis by the Network Method, *Trans. ASME*, vol. 78, no. 4, pp. 725–735, 1956.
- [14] EnergyPlus Documentation-Engineering Reference, Version 8, Chap. 3, Ernest Orlando Lawrence Berkeley National Laboratory, University of California, Berkeley, CA, 2013.
- [15] W. W. Yuen and E. E. Takara, Development of a General Zonal Method for Analysis of Radiative Transfer in Absorbing and Anisotropically Scattering Media, *Numer. Heat Transfer B*, vol. 25, pp. 75–96, 1994.
- [16] F. Liu, Numerical Solutions of Three-Dimensional Non-Grey Gas Radiative Transfer Using the Statistical Narrow-Band Model, *J. Heat Transfer*, vol. 121, no. 1, pp. 200–203, 1999.
- [17] P. J. Coelho, Numerical Simulation of Radiative Heat Transfer from Non-Gray Gases in Three-Dimensional Enclosures, *J. Quant. Spectrosc. Radiat. Transfer*, vol. 74, no. 3, pp. 307–328, 2002.
- [18] G. El Hitti, M. Nemer, and K. El Khoury, Reducing CPU Time for Radiative Exchange and Transient Heat Transfer Analysis Using Zone Method, *Numer. Heat Transfer, Part B Fundam*, vol. 56, no. 1, pp. 23–37, 2009.
- [19] W. M. G. Malalasekera and E. H. James, Thermal Radiation in a Room: Numerical Evaluation, *Build. Serv. Eng. Res. Technol.*, vol. 14, no. 4, pp. 159–168, 1993.
- [20] B. A. Price and T. F. Smith, Thermal Response of Composite Building Envelopes Accounting for Thermal Radiation, *Energy Convers. Manage.*, vol. 36, no. 1, pp. 23–33, 1995.
- [21] W. W. Yuen, RAD-NNET, A Neural Network Based Correlation Developed for a Realistic Simulation of the Non-Gray Radiative Heat Transfer Effect in Three-Dimensional Gas-Particle Mixtures, *Int. J. Heat Mass Transfer*, vol. 52, no. 13, pp. 3159–3168, 2009.
- [22] W. L. Grosshandler, RADCAL, A Narrow-Band Model for Radiation Calculations in a Combustion Environment, NIST-TN-1402, Maryland, 1993.
- [23] W. W. Yuen, W. C. Tam, and W. K. Chow, Assessment of Radiative Heat Transfer Characteristics of a Combustion Mixture in a Three-Dimensional Enclosure Using RAD-NETT (With Application to a Fire Resistance Test Furnace), *Int. J. Heat Mass Transfer*, vol. 68, pp. 383–390, 2014.
- [24] W. C. Tam, Analysis of Heat Transfer in a Building Structure Accounting for the Realistic Effect of Thermal Radiation Heat Transfer, PhD Dissertation, Mechanical Engineering Dept., The Hong Kong Polytechnic University, Hong Kong, China, 2013.
- [25] R. Siegel and J. R. Howell, *Thermal Radiation Heat Transfer*, 4th ed., chap.13, Taylor and Francis, New York, 2002.
- [26] Fluent Inc., Fluent User's Guide Version 14.0., Fluent Inc., Lebanon, 2011.
- [27] G. N. Walton, Thermal Analysis Research Program Reference Manual, NBSIR 83-2655, U.S. Department of Commerce, 1983.
- [28] R. Zhang, K. P. Lam, S. C. Yao, and Y. C. Zhang Coupled EnergyPlus and Computational Fluid Dynamics Simulation for Natural Ventilation, *Build. Environ.*, vol. 68, pp. 100–113, 2013.

Appendix A: The effect of one-zone approximation on prediction of indoor air temperature: comparison between zonal model and CFD

A numerical analysis is carried out to investigate the influence of one-zone, well-mixed approximation on the simulation accuracy of interior convective heat transfer and resulting indoor air temperature. Simulations are conducted with BERHT (zonal model) and a commercially available CFD package (Fluent [26]) for an enclosure similar to that shown in Figure 1. The enclosure is considered to be a passive closed system, so infiltration, ventilation, and/or HVAC systems will not be included. To facilitate the comparison with CFD results, the medium is considered to be transparent to thermal radiation. Without external sources (i.e., pumps, fans, etc.), natural convection is thus the primary heat transfer mechanism between the surfaces and the indoor air. In BERHT, the convective heat transfer between a surface and the zone air is governed by the Newton's cooling law:

$$q'' = h(T_s - T_z) \quad (A1)$$

where q'' is the convective heat flux, T_s is the averaged temperature for the surface, and T_z is the averaged temperature of indoor air (zone air). The convective heat transfer coefficient, h , can be modeled

Table A1. Correlations for natural convection used in BERHT [14].

| Surface | Correlation | Remarks |
|------------|---|---------------------|
| Vertical | $h = 1.310 T_s - T_a ^{1/3}$ | – |
| Horizontal | $h = \frac{9.482 T_s - T_a ^{1/3}}{7.283 - \cos(\Sigma) }$ | Enhanced convection |
| Horizontal | $h = \frac{1.810 T_s - T_a ^{1/3}}{1.382 + \cos(\Sigma) }$ | Reduced convection |

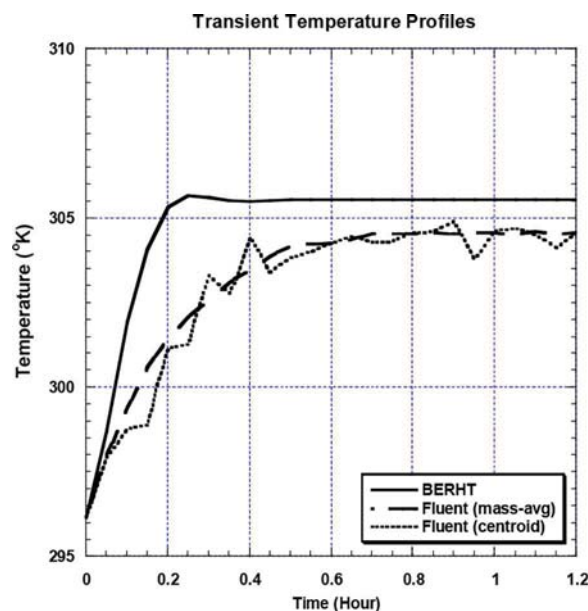
Notes: Σ is the tilted angle of the surface. (For floor surface, Σ is at 180° and for roof surface, Σ is at 0°).

by either a SIMPLE [27], TARP [27], or adaptive convection algorithm [6]. Previous studies [28] demonstrated that all three algorithms generate similar heat transfer coefficients for interior surfaces. Thus, the default convection algorithm used in EnergyPlus, TARP, is utilized in this numerical analysis. The correlations are summarized in Table A1 and are in the function of surface orientation and the difference between surface and indoor air temperature.

In Fluent, simulation is conducted to obtain detailed information of air in the enclosure. Standard energy and k-epsilon models are used to solve the energy and mass balance for air in the enclosure. The heat capacity, thermal conductivity, and dynamic viscosity of air are assumed to be constant and are evaluated at 296.15°K . The air density is determined using the incompressible idea gas relation. The enclosure interior is discretized using structured hexahedral grids with a fine grid of 562,800 cells. For solution methods, a second-order upwind scheme is used for the discretization of the convective terms in transport equations in order to reduce numerical diffusion. The body force weighted scheme is used for discretization of pressure and the PISO algorithm is used for the pressure–velocity coupling.

In both models, fixed boundary conditions are imposed on all surfaces. Each surface is assumed to be maintained at a constant temperature of 325°K with the remaining surfaces kept at 300°K . Initially, the indoor air is maintained at 296.15°K in 1 atm. Both simulations are run for 24 h with a time step of 180 s.

Transient and steady-state indoor air temperature profiles are generated and are shown in Figures A1 and A2, respectively. In Figure A1, the air temperature obtained from BERHT and localized (at centroid) air temperature and mass averaged air temperature obtained from Fluent are presented. In Figure A2, the steady-state zone/indoor air temperature distributions for three different directions are presented. The indoor air temperature distributions along the x -, y -, and z -axes are obtained at

**Figure A1.** Transient temperature profile of indoor air obtained from BERHT and Fluent.

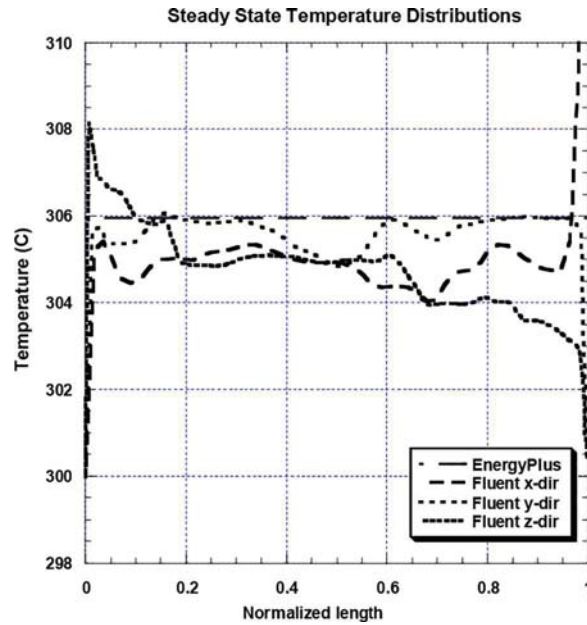


Figure A2. Steady-state temperature distributions of indoor air obtained from BERHT and Fluent.

the center of planes YZ, XZ, and XY, respectively. Results show that the air temperature distribution across the simulation domain are not uniform. The assumption of a uniform temperature within the enclosure is thus not valid. As shown, the rate of temperature increase at the beginning of simulation in BERHT data is about twofold that observed from the Fluent results. The air temperature takes about 0.4 and 0.8 h to reach steady-state condition for BERHT and Fluent, respectively. This suggests that it would take twice as long for the heat from the surrounding surfaces to be completely dispersed to the air when detailed fluid transport is considered. Physically, this thermal penetration effect will occur only with radiative heat transfer in an absorbing/emitting medium. But due to the well-mixed approximation, the one-zone model introduces this effect in its temperature prediction erroneously. The effect of the radiative absorption effect, which is of the same order of magnitude as the convective effect, is thus difficult to visualize in a one-zone approximation. Nevertheless, the radiative effect is physically important and some correction must be made to the one-zone approximation to demonstrate more effectively the relative importance of the convective and radiative heat transfer effect. Such a task is current under consideration and will be reported in future publications.

Appendix B: A numerical analysis on the influence of the effect of the external heat transfer and boundary conditions on the profile of overall heat transfer and zone air temperature distribution

The lack of impact of radiative heat transfer on the profile of the overall heat transfer and the zone air temperature under current consideration can also be understood by noting that these parameters are not only controlled by the internal heat transfer mechanisms, they are also influenced by external heat transfer and boundary conditions such as solar irradiation, wind speed, and surrounding temperatures. To illustrate this interaction systematically, a series of simulations were conducted for a transparent medium with the internal convective heat transfer being modified by a multiplicative factor. Results for total heat transfer to the zone air and the corresponding zone air temperature for different multiplicative factors (0.1 and 0.01 for reduction in convection, and 2 and 10 for increase in convection) are shown in Figures B1 and B2. It is interesting to note that over a wide range of changes in the convective heat transfer effect (factor of 1/10, 2, and 10), heat transfer to the zone air and the corresponding air

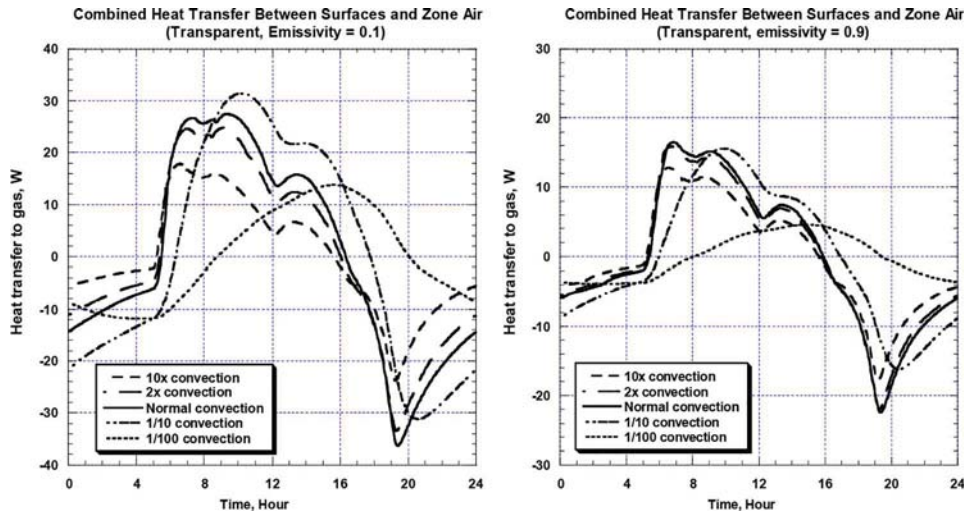


Figure B1. Total heat transfer to the zone air for different levels of internal convection heat transfer in different interior surface configurations.

temperature do not vary significantly. The effect of reduced convection is significant only when the multiplicative factor is 1/100.

Results from Figures B1 and B2 are important from the perspective of assessing the effect of radiative heat transfer, because the order of magnitude of the radiative heat transfer effect can be estimated by an equivalent radiative heat transfer coefficient, $4\sigma T_w^3$. For $T_w \sim 300$ K, the equivalent heat transfer coefficient is approximately $6 \text{ W/m}^2\text{-K}$, which is of the same order as the convective heat transfer coefficient used in EnergyPlus and BERHT as given by Table A1. The radiative heat transfer effect is therefore in the order of increasing the convective heat transfer by a factor between 2 to 5. As shown in Figures B1 and B2, this enhancement is insufficient to cause significant changes on the profile of total heat transfer and the resulting zone air temperature. As demonstrated in the main text, the effect of radiation is thus not apparent from the behavior of the zone temperature. The impact is significant only on the distribution between radiative heat transfer and convective heat transfer of the individual boundary.

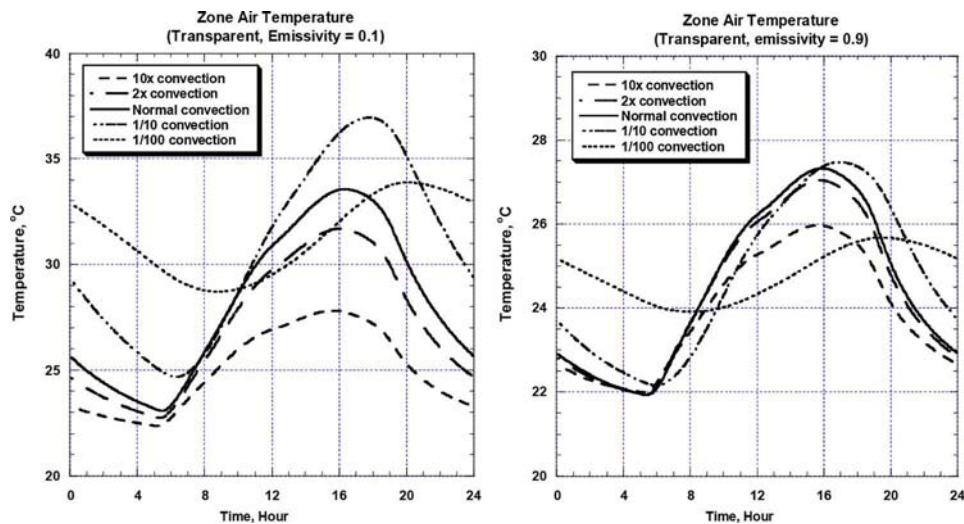


Figure B2. Temperature of the zone air for different levels of internal convective heat transfer in different interior surface configurations.